High-yield Magnetic Recoil neutron Spectrometer on the National Ignition Facility for operation up to 60 MJ

M. Gatu Johnson[1,a)], T.M. Johnson[1], B.J. Lahmann[1], F.H. Séguin[1], B. Sperry[1], N. Bhandarkar[2], R.M. Bionta[2], E. Casco[2], D.T. Casey[2], A.J. Mackinnon[2], N. Masters[2], A. Moore[2], A. Nikroo[2], M. Hoppe[3], R. Mohammed[3], W. Sweet[3], C. Freeman[4], V. Picciotto[4], J. Roumell[4] and J.A. Frenje[1]

[1]*Massachusetts Institute of Technology, Cambridge, Massachusetts 02139, USA*
[2]*Lawrence Livermore National Laboratory, Livermore, California 94550, USA*
[3]*General Atomics, San Diego, California 92186, USA*
[4]*State University of New York at Geneseo, Geneseo, New York 14454, USA*

(Presented XXXXX; received XXXXX; accepted XXXXX; published online XXXXX)

Recent progress at the National Ignition Facility, with neutron yields now of order 1e17, places new constraints on diagnostics employed to characterize implosion performance. The Magnetic Recoil neutron Spectrometer (MRS), routinely used to measure yield, ion temperature (T_{ion}) and down-scatter ratio (*dsr*), has been adapted to allow measurements of *dsr* up to a yield of 5e17, yield and T_{ion} up to a yield of 2e18 in the near term with new data processing techniques and conversion foil solutions. This paper presents a solution for extending MRS operation up to a yield of 2e19 (60 MJ) by moving the spectrometer outside of the NIF shield wall. This will not only enhance the upper yield limit 10x, but also improve signal-to-background 5x.

I. INTRODUCTION

Yields from cryogenically layered deuterium-tritium (DT) inertial confinement fusion (ICF) implosions at the National Ignition Facility (NIF) are reaching new records of order 1e17,[1] ushering in an era of unprecedented opportunities and challenges for the instruments used to diagnose ICF plasmas. NIF neutron spectrometers are used to provide[2] the critical performance parameters of neutron yield, ion temperature (T_{ion}, inferred from the width of the primary 14-MeV neutron spectrum[3,4,5]), and areal density (through the downscatter ratio, *dsr,* calculated[6] as the ratio of the neutron yield in the energy ranges 10-12 MeV to 13-15 MeV).

One of the NIF neutron spectrometers is the magnetic recoil neutron spectrometer (MRS; FIG. 1).[7-8] Prior to the recent record experiments, MRS allowed operation up to a ceiling yield of ~9e16. This paper discusses how adapting CR-39 processing and analysis techniques (Sec. II) and the use of smaller foils (Sec. III) have allowed an increase in this ceiling to 2e18 in the short term. Two different foil configurations are considered; a stand-alone foil at 26cm from the implosion, and a glow-discharge-polymer deposited foil fielded on the hohlraum for significantly improved resolution.[9-10] For the hohlraum foils, challenges due to uncontrolled foil motion, foil oxygen uptake, and background *n,d* reactions are discussed, and potential solutions proposed. The smaller foils come with reduced efficiency, detrimentally impacting signal-to-background (S/B).[11] In the current configuration, MRS *dsr* data are likely to be compromised at yields >5e17. This paper also proposes a solution to this problem: moving the MRS behind the outer NIF shield wall (Sec. IV). MCNP simulations predict an increase in the *dsr* yield limit to ~2e19 for this proposed configuration.

[a)]Author to whom correspondence should be addressed: gatu@psfc.mit.edu.

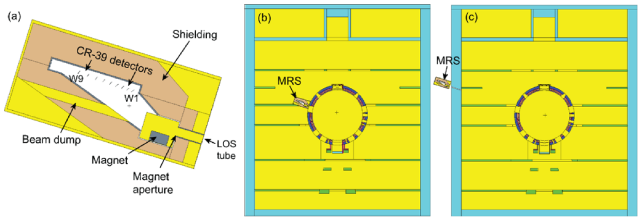

FIG. 1. (Color online). (a) MCNP model of the NIF MRS with the detector components indicated, (b) in its current location on the NIF target chamber, and (c) in its proposed new location outside of the shield wall.

II. OPERATION LIMITS OF THE CURRENT NIF MRS

MRS consists of a deuterated plastic (CD) foil positioned close to the implosion, a permanent Ne-Fe-B magnet behind a fixed-size aperture outside of the target chamber wall, and an array of CR-39 detectors in the magnet focal plane. A fraction of the neutrons from an ICF implosion scatter elastically in the CD foil generating recoil deuterons, which are subsequently momentum separated in the magnet to end up in a different physical location on the detector array depending on their energy. The neutron spectrum is inferred from the measured recoil deuteron energy spectrum using a response function calculated based on the well-known *n,d* elastic scattering cross section and

the geometry of the setup. The MRS setup can be adapted to the predicted yield of an experiment by changing the CD foil;[5] the current lowest efficiency/highest resolution configuration available is a 50-μm thick, 3 cm^2 active area foil giving an efficiency of 4.4e-12 deuteron tracks/source neutron and a FWHM resolution of 0.43 MeV (henceforth referred to as the "high yield configuration").

The upper yield limit for MRS operation depends on the density of tracks on the CR-39 coupons used in the detector array.[12] At the nominal 6h etch time, a rule-of-thumb is that the track density should be $<1.5\times10^4$ cm^{-2}. As the track overlap limit scales with the square of the track size,[12] which in turn scales with etch time,[13] this upper limit can be increased by reducing the etch time of the CR-39 coupons. For the exposure and etch conditions of the NIF MRS CR-39, it is found that a minimum etch time of 1.25h is required for all signal tracks to be developed. A small amount of track overlap can be corrected for in the analysis by identifying ellipsoidal tracks likely to represent overlapping tracks, and double-counting these tracks. Using the two methods of short etch time and overlap correction combined, MRS has been successfully operated up to a track density of 5×10^5 cm^{-2}, corresponding to a neutron yield limit of $\sim5\times10^{17}$ in the standard high yield configuration. (Average track diameter in the primary peak for NIF MRS at 6h etch is 8.2 μm, 1.25h etch 2.3 μm.)

A. Background considerations

Two types of background must be considered when analyzing NIF MRS data: intrinsic (due to CR-39 defects) and neutron-induced (due to neutrons knocking out charged particles in the CR-39). The intrinsic background varies significantly between pieces of CR-39 and with analysis conditions, in particular darkness (i.e., contrast) of tracks considered in the analysis.[14] An average value at contrast c<13% is 199±165 cm^{-2}, with the large 1σ error bar capturing the substantial piece-to-piece variations observed. The average increases to 942 at c<35% and 6930 at c<65%. The neutron-induced background also varies with analysis conditions and additionally with neutron energy and etch time. Typical CR-39 neutron detection efficiencies at 6h etch for c<35% and eccentricity e<35% are $(6.0\pm0.7)\times10^{-5}$ per incident neutron for 14-MeV DT neutrons and $(1.1\pm0.2)\times10^{-4}$ per incident neutron for 2.5-MeV DD neutrons.[15] To allow determination of the expected neutron background in the NIF MRS data, the neutron fluence per source neutron on the MRS detector is calculated using the MCNP code,[16] with the model shown in Fig. 1 and the result shown in Fig. 2. As an example of the expected balance of intrinsic vs neutron-induced background and as a check of the validity of the MCNP model, consider the MRS data measured on CR-39 detector #8 from NIF experiment N210808, etched for 6h. The total analyzed area on this piece of CR-39 is 28 cm^2. 4005 signal tracks are isolated by (i) limiting the accepted tracks to c<13%, e<15%, and diameter 7<d<10.2 μm and (ii) subtracting a uniform background, inferred from the observed tracks in the background region (which could be intrinsic or neutron-induced), scaled up to the full piece, of 38900 tracks. With this CR-39 area and contrast limit, the expected intrinsic background level is ~5600 tracks, and thus a factor 7 lower than the neutron-induced background in this particular case. With the simulated background neutron fluence of 1.3e-9 on W8 (Fig. 2), the yield on this shot of 4.54e17, and the expected CR39 efficiency for DT neutrons of 6e-5, the predicted neutron background at c<35% and e<35% is ~1e6. While this is substantially higher than the 3.3e4 inferred for the tighter track diameter bounds used above, if the c and e limits in the analysis are both relaxed to 35%, a total background of 1.4e6 is instead found on this detector. Considering that the CR-39 neutron detection efficiency increases with decreasing neutron energy and that the average neutron energy is well below 14 MeV (Fig. 2b), this roughly agrees with the prediction, with the data supporting the validity of the MCNP result.

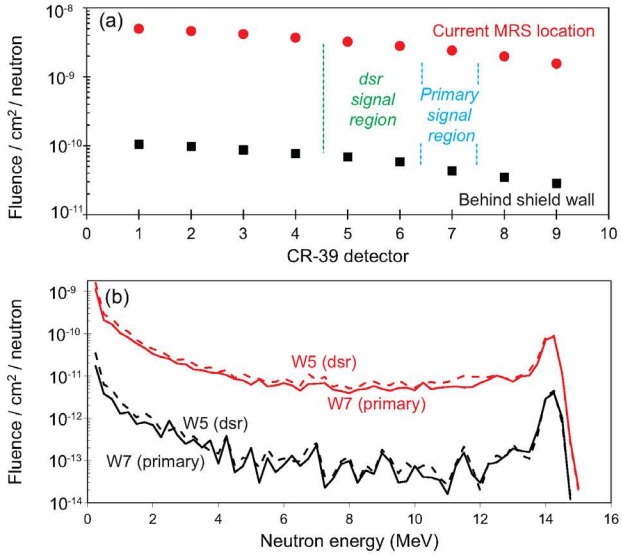

FIG. 2. (Color online). (a) MCNP-calculated neutron background fluence per produced neutron on each CR-39 piece in the MRS detector, for the current configuration (red circles) and proposed location outside of the NIF shield wall (black squares). The error bars are smaller than the symbols. (b) MCNP-simulated neutron background spectra for the primary detector (W7, solid lines) and *dsr* detector (W5, dashed lines), again with the current configuration in red and the proposed outside-of-shield-wall configuration in black.

As discussed in Ref. [11], any background that is uniform across the CR-39 can be straightforwardly subtracted in the analysis of the data on each individual CR-39 detector. However, the neutron-induced background across the CR-39 in the *dsr* region of the MRS spectrum in the current configuration is found to be non-uniform. This background was measured on two shots, N130628 and N151020, with MRS fielded without a CD conversion foil and with neutron yields of 1.6e15 and 3.5e15, respectively (Fig. 3a). MRS data are corrected for this by scaling the empirically measured background by the neutron yield on each new shot and subtracting before inferring a *dsr*

number, as shown in Fig. 3b. Note that at the recent high yield levels, this background is extrapolated by two orders of magnitude, raising questions about the accuracy of features of the component, in particular the fall-off and shape of its high-energy tail, which was at the noise level at 3.5e15 yield. Background data should be obtained at higher yield in the near term to check this. The 10-12 MeV neutron energy range of interest in the *dsr* calculation approximately corresponds to 8.9-10.7 MeV deuteron energy (E_d). As can be seen in Fig. 3b, the ratio of the non-uniform neutron background (green triangles) to signal (blue diamonds) in this energy range varies from ~1:1 to 4:1. Reducing MRS efficiency without also improving S/B will linearly drop the signal while keeping the background the same; such efficiency reduction will clearly compromise the *dsr* measurement. Given this constraint, the *dsr* upper yield limit for the current MRS is estimated to be 5e17.

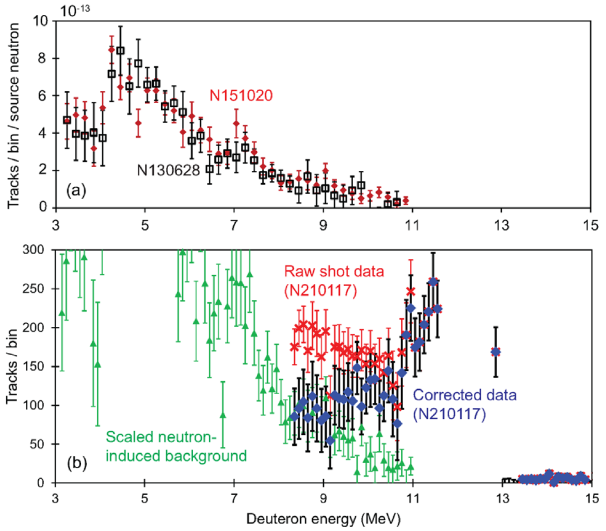

FIG. 3. (Color online). (a) Non-uniform neutron-induced background, normalized by the neutron yield, measured on two shots with MRS fielded without a CD conversion foil: N130628 and N151020. The results from the two shots are seen to track each other closely. (b) MRS data from shot N210117, with MRS fielded in the high standard high yield configuration, shown raw (red crosses) and corrected (blue diamonds) for the neutron-induced background scaled up to the N210117 yield (green triangles). (Note that the CR-39 detectors covering the energy range 3-8 MeV were not fielded on N210117.)

Given that the background scales directly with neutron yield, there will also be an upper yield limit where MRS data saturates on neutron background alone. Assuming a max acceptable track density of 5×10^5 cm^{-2} and a total CR-39 neutron detection efficiency of 6e-5, this limit for the primary data on W7 will be ~3.5e18.

The other new consideration impacting MRS analysis at yields >1e17 is that the coincidence counting technique[17] (CCT) previously used to eliminate intrinsic and reduce neutron-induced background in the MRS analysis fails. The reason for this is that the number of random coincidences scales with track density squared; at 1e17 yield, the track density on MRS becomes high enough where the CCT background overtakes the background inferred from standard, front side CR-39 counting (SCT). The use of SCT means that the analysis becomes susceptible to gradients in intrinsic background, which now has to be subtracted assuming it is uniform across the piece. Comparison of CCT and SCT analysis over a range of implosions has been undertaken to verify that the two methods agree on average, while the SCT results scatter up and down around the established CCT result depending on shot. This is concluded to result from variations in intrinsic noise gradients, and leads to larger uncertainty in the *dsr* numbers inferred from SCT than from CCT analysis.

III. REDUCING EFFICIENCY I: THE FOIL METHOD

A short-term solution to avoiding saturation at high yield is to reduce the MRS efficiency by reducing the number of deuterons available for *n,d* scattering in the foil. As discussed above, this will quickly lead to an S/B problem in the *dsr* measurement, but it will facilitate primary yield and T_{ion} measurements up to a higher upper yield limit than previously possible. With MRS expected to saturate on background alone at ~3.5e18 as discussed above, it is reasonable to aim for an upper yield limit of 2e18 when designing the new foil configuration.

As discussed in Ref. [5], two methods exist for manufacturing MRS foils: (i) the hot-press method, used to make stand-alone CD_2 foils down to 50 μm thickness, and (ii) the glow discharge polymer deposition (GDP) method, which can be used to make arbitrarily thin foils. The GDP foils have been found to degrade rapidly with time when used on more than one shot, and also to delaminate from the backer they are deposited onto, and are thus not feasible for repeated use. Hence, the standard MRS foils fielded at 26 cm from the implosions are all made using the hot-press method. Since MRS already uses the minimum thickness available for this foil type, the path forward to reduced efficiency is to reduce the foil area. The easiest way to achieve this is to add a rear aperture between the foil and the MRS detector, thick enough to range down any deuterons born behind it (Fig. 4). The high yield configuration currently fielded with MRS uses a 3 cm^2, 250-μm thick Ta rear aperture. A new aperture has been designed and manufactured (Fig. 4c) with a 0.5cm^2 area, which will reduce the foil effective area and hence MRS efficiency by a factor 6, bringing the MRS upper yield limit to 2e18 (or 6 MJ).

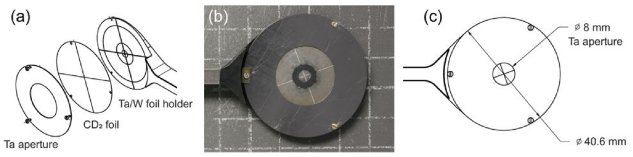

FIG. 4. (a) Cartoon of 250-μm thick Ta aperture fielded behind the CD foil on the MRS foil holder to reduce effective foil area, hence instrument efficiency, (b) a picture of the foil assembly from shot N210117, and (c) a new, reduced-size aperture design, which will reduce the efficiency a further factor of 6.

A promising technique for substantially improving resolution in the MRS measurements at maintained efficiency is fielding a smaller foil closer to target chamber center (TCC). As discussed in Ref. [10], this works because the ion optical broadening of the signal is much reduced with the smaller MRS foil. On NIF indirect drive implosions, this is achieved by fielding the foil on the hohlraum.[9] The foils used in this configuration, which are single use by definition, are all made by the GDP method, which conveniently allows them to be deposited directly onto a backer without the use of glue. MCNP and Geant4[18] simulations show that fielding a 0.4 mm diameter, 40-μm thick foil on the hohlraum will improve the resolution nearly 2x compared to standard high yield operation (240 keV vs 430 keV FWHM) and reduce systematic uncertainty in inferred T_{ion} 4x (0.44 keV vs 0.11 keV) at nearly identical efficiency (4.4e-12 vs 3.8e-12 signal tracks/source neutron). The foil-on-hohlraum technique can also easily be adapted for higher yield by reducing foil area and thickness, and will be required for the next-generation time-resolved neutron spectrometer, MRSt, which is currently under development.[9,19] However, tests fielding MRS in this configuration undertaken on high-yield NIF implosions N190918, N191007, N200125, N200229 and N200308 identified three issues that must be resolved before this technique becomes broadly applicable. These include (i) interference in the *dsr* region from *n,d* reactions in the hohlraum diagnostic band, (ii) foil movement prior to bang time, and (iii) uncharacterized oxygen content in the foils.

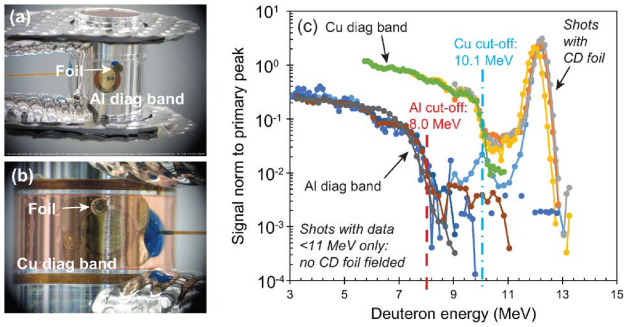

FIG. 5. (Color online). MRS CD foil fielded on (a) an Al diagnostic band and (b) a Cu diagnostic band hohlraum. In (c), neutron yield-normalized MRS deuteron spectra for both configurations and for MRS fielded with and without the CD foil are compared. As indicated by this data, *n,d* reactions in the diagnostic band give rise to a background component which interferes in the *dsr* region in the Cu case.

Fig. 5 shows MRS data from shots with and without a GDP foil fielded on hohlraums with Al or Cu diagnostic bands. The peak at deuteron energy E_d~12.5 MeV is caused by the primary DT neutron peak. The large background structures at E_d<8.0 MeV in the Al band and E_d<10.1 MeV in the Cu band cases do not appear in MRS data with the foil fielded on a foil holder at the standard 26 cm standoff, but arise in the hohlraum case even when MRS is fielded without a foil. Both Al and Cu have non-negligible but poorly characterized cross sections[20] for *n,d* reactions; ^{27}Al(*n,d*)^{26}Mg has σ~0.02 b for 14-MeV neutrons and a Q-value of -6.0 MeV, consistent with the upper energy cut-off of 8.0 MeV, and ^{63}Cu(*n,d*)^{62}Ni has σ~0.01 b and a Q-value of -3.9 MeV, consistent with the upper energy cut-off of 10.1 MeV. As a reminder, the E_d scale *dsr* region equivalent is ~8.9-10.7 MeV, which means this background virtually prevents inference of *dsr* when the foil is fielded on a Cu band hohlraum. A solution to this problem is to always field the MRS foil on a patch of Al or other material that does not generate deuterons in the *dsr* region.

When comparing MRS-measured yield and T_{ion} from these implosions with yields measured by neutron activation detectors[21] (NAD) and T_{ion} measured with neutron time-of-flight (nTOF) spectrometers,[22] MRS yield was found to vary from 75-100% of NAD and T_{ion} from 0.4-1.5 keV above the average nTOF value. These differences are consistently explained by uncontrolled foil motion prior to burn, randomly ejecting and tilting the foil, reducing efficiency and increasing resolution compared to nominal. Impact simulations of the hohlraum load confirm that fielding the foil on the edge of a hohlraum diagnostic window makes it susceptible to such motion. These simulations also suggest that this problem can be solved by fielding the foil on an Al tab, which the target fabrication team confirms would be a straightforward modification.

The final GDP foil problem is that this material is known to be susceptible to oxygen uptake,[23-24] which has not been well characterized. This will impact the MRS resolution; unless corrected for in the response function simulations, it will introduce an error in inferred T_{ion}.[10] Rutherford Backscattering (RBS) experiments using 3 MeV protons generated by the Geneseo Pelletron accelerator are underway to characterize the foil impurities, which if known can be straightforwardly accounted for in the analysis. Preliminary analysis of the RBS data (Fig. 6) suggests that both nitrogen and oxygen impurities are present in the foils.

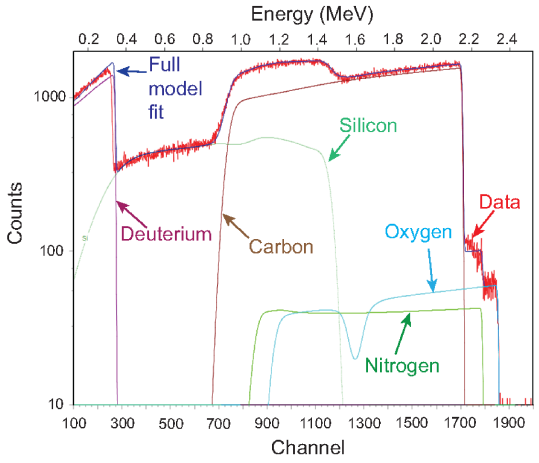

FIG. 6. (Color online). Result from a Rutherford Backscattering experiment of a CD sample deposited onto an Si backer. The data (red) is found to be best described by a full model (dark blue) considering the known Si, C and D content in the sample and assuming a combination of O (1.4% atomic) and N (1.2% atomic) impurities in the foil.

IV. REDUCING EFFICIENCY II: FIELDING BEHIND SHIELD WALL

Longer term, higher yields than 2e18 are expected at the NIF, requiring reduction also of the MRS background. This can be achieved by moving the MRS to behind the NIF shield wall (Fig. 1), i.e., moving the magnet aperture from the current 596 cm to 1866 cm from TCC. Since the signal efficiency scales inversely with distance squared, this means ~10x reduction in efficiency. Specifically, efficiency simulations using MCNP with a 50-μm thick, 3 cm^2 active area foil fielded 26 cm from TCC indicates a reduction from 4.4e-12 signal tracks/source neutron in the current location to 4.1e-13 tracks/neutron in the proposed new location. The superiority of the shield wall for reducing neutron-induced background leads to a relatively bigger reduction in neutron-induced background fluence (see Fig. 2), from 2.4e-9 to 4.3e-11 per cm^2 and source neutron in the primary peak; this means the expected S/B improvement is ~5.2x. With the previous expected primary overlap limit of 2e18 for the 0.5 cm^2 effective foil area and *dsr* overlap limit of 5e17 due to S/B considerations, the new yield limit for *dsr* can be expected to be ~2e19 (or 60 MJ) at maintained S/B. In addition, fielding MRS outside the shield wall is also expected to eliminate the issue with non-uniform background (Fig. 3), further simplifying background subtraction and improving data quality. Such an upgrade would also improve capability of MRS for measuring low-level features at the high end of the primary DT peak, which can be used to assess the impact of alpha heating in these experiments;[25] such a high-level feature is just starting to be discernible above background in the current high-yield configuration on the highest yield shots with 30x yield amplification due to alpha heating.

V. CONCLUSIONS

With the new era of yields of order 1e17 obtained at the NIF, diagnostics need to adapt to continue to provide key measurements to assess implosion performance. In this paper, it is shown that with small modifications, the MRS neutron spectrometer upper yield limit has been extended to 2e18 for primary (yield and T_{ion}) measurements and 5e17 for *dsr*. Measurements can also be undertaken at improved resolution by fielding the MRS foil on the hohlraum, provided the hohlraum is modified to eliminate (i) interference in the *dsr* region from diagnostic band *n,d* reactions and (ii) uncontrolled foil motion prior to burn, and provided impurity content in the foils is well characterized. MCNP simulations show that moving the MRS outside the shield wall would allow a further extension of the upper yield limit to 2e19 for both primaries and *dsr*, and also facilitate improved measurements of weaker spectral features, including a feature on the high-energy end of the DT peak expected to correlate with alpha heating, at current yields due to a 5.2x improvement in S/B.

VI. ACKNOWLEDGMENTS

This work was supported in part by the U.S. Department of Energy NNSA MIT Center-of-Excellence under Contract DE-NA0003868, and by Lawrence Livermore National Laboratory under Contract B640112. This report was prepared as an account of work sponsored by an agency of the United States Government. Neither the United States Government nor any agency thereof, nor any of their employees, makes any warranty, express or implied, or assumes any legal liability or responsibility for the accuracy, completeness, or usefulness of any information, apparatus, product, or process disclosed, or represents that its use would not infringe privately owned rights. Reference herein to any specific commercial product, process, or service by trade name, trademark, manufacturer, or otherwise does not necessarily constitute or imply its endorsement, recommendation, or favoring by the United States Government or any agency thereof. The views and opinions of authors expressed herein do not necessarily state or reflect those of the United States Government or any agency thereof.

VII. DATA AVAILABILITY

The data that support the findings of this study are available from the corresponding author upon reasonable request.

VIII. REFERENCES

[1] A.B. Zylstra et al., Nature 601, 542 (2022).
[2] M. Gatu Johnson et al., Rev. Sci. Instrum. 83, 10D308 (2012).
[3] L. Ballabio, J. Källne, and G. Gorini, Nucl. Fusion 38, 1723 (1998).
[4] R. Hatarik et al., J. Appl. Phys. 118, 184502 (2015).
[5] M. Gatu Johnson et al., Rev. Sci. Instrum. 87, 11D816 (2016).
[6] J. A. Frenje et al., Nucl. Fusion 53, 043014 (2013).
[7] J.A. Frenje et al., Phys. Plasmas 17, 056311 (2010).
[8] D.T. Casey et al., Rev. Sci. Instrum. 84, 043506 (2013).
[9] C.E. Parker et al., Rev. Sci. Instrum. 89, 113508 (2018).
[10] M. Gatu Johnson et al., Rev. Sci. Instrum. 92, 023503 (2021).
[11] M. Gatu Johnson et al., Rev. Sci. Instrum. 85, 11E104 (2014).
[12] A. Zylstra et al., Nucl. Instrum. Methods Phys. Res. A 681 (2012).
[13] F.H. Séguin et al., Rev. Sci. Instrum. 74, 975 (2003).
[14] R. Przobocki et al., Rev. Sci. Instrum. 92, 013504 (2021).
[15] J.A. Frenje et al., Rev. Sci. Instrum. 73, 2597 (2002).
[16] MCNP6.2, https://mcnp.lanl.gov/.
[17] D.T. Casey et al., Rev. Sci. Instrum. 82, 073502 (2011).
[18] S. Agostinelli et al., Nucl. Instrum. Methods Phys. Res. A 506(3), 250 (2003).
[19] J.A. Frenje et al., Rev. Sci. Instrum. 87, 11D806 (2016).
[20] https://www-nds.iaea.org/exfor/
[21] D.L. Bleuel et al., Rev. Sci. Instrum. 83, 10D313 (2012).
[22] T. J. Clancy et al., in Target Diagnostics Physics and Engineering for Inertial Confinement Fusion III, edited by P.M. Bell and G. P. Grim, SPIE Proc. Vol. 9211 (SPIE, Bellingham, 2014).
[23] T.R. Gengenbach, Z.R. Vasic, and R.C. Chatelier, J. Poylmer Science: Part A 32, 1399 (1994).
[24] H. Reynolds, S. Baxamusa, S. W. Haan, P. Fitzsimmons, L. Carlson, M. Farrell, A. Nikroo and B.J. Watson, J. Appl. Phys. 119, 085305 (2016).
[25] J. Källne et al., Phys. Rev. Lett. 85, 1246 (2000).